MODELING FERROFLUIDS IN SPATIALLY-TRAVELING SINUSOIDALLY TIME-VARYING MAGNETIC FIELDS

Leidong MAO and Hur KOSER
Department of Electrical Engineering, Yale University, 15 Prospect Street, New Haven, CT 06511, USA*

Ferrofluids are stable colloidal suspensions of nanosize ferromagnetic particles in either an aqueous or an oil-based solvent[1]. In the presence of a magnetic field gradient within a ferrofluid, magnetic forces and torque are developed to drive magnetic particles, which subsequently draw along the liquid solvent carrier. This allows continuous actuation and precise positioning of the ferrofluid using a magnetic field. Ferrofluids have found their way into a variety of applications, such as sealing, damping[2] and blood separation[3]. In this study, we present a numerical method to simulate the dynamics of ferrofluids in spatially-traveling, sinusoidally time-varying magnetic fields. Actuation using traveling waves involves magnetic body forces and torque on the magnetic moment of nanoparticles, both of which affect the overall pumping.

1. INTRODUCTION

Ferrohydrodynamic pumping in spatially uniform, sinusoidally time-varying magnetic fields has been studied extensively in the past[4]. Here we examine a different case where the applied sinusoidal field is a spatially traveling wave. The importance of traveling wave magnetic fields lies in the fact that they will develop both magnetic body forces and magnetic torque in the ferrofluid; these two effects need to be considered simultaneously to determine ferrofluid pumping.

In this study, the motion of a ferrofluid in a traveling wave magnetic field is investigated in the most general case. A second order central-differencing scheme is employed iteratively to calculate the magnetic field strength inside the ferrofluid, as well as the flow and spin velocities of magnetic particles.

2. GOVERNING DYNAMICS

2.1. Magnetization constitutive law

The magnetization relaxation equation[1] for a ferrofluid with simultaneous magnetization, convection with position dependent velocity $\mathbf{v}$, and reorientation due to particle spin $\boldsymbol{\omega}$ is

$$\frac{\partial \mathbf{M}}{\partial t} + (\mathbf{v} \cdot \nabla)\,\mathbf{M} - \boldsymbol{\omega} \times \mathbf{M} + \frac{1}{\tau}\left[\mathbf{M} - \chi_0 \mathbf{H}\right] = 0 \tag{1}$$

*This work is funded by Yale University.

where τ is a relaxation time constant and χ_0 is the effective magnetic susceptibility. In this work, the magnetic susceptibility is taken to be a constant. $\mathbf{M}$ is the magnetization and $\mathbf{H}$ is the magnetic field vector. In our modeling, we are considering a cylindrical ferrofluid section as shown in Figure 1. By symmetry, the flow velocity has only a z-directed component and the particle angular velocity has only a θ-directed component. Both velocities will change with the r coordinate, i.e.

$$\mathbf{v} = v_z(r)\mathbf{i_z} \quad \boldsymbol{\omega} = \omega_\theta(r)\mathbf{i}_\theta \tag{2}$$

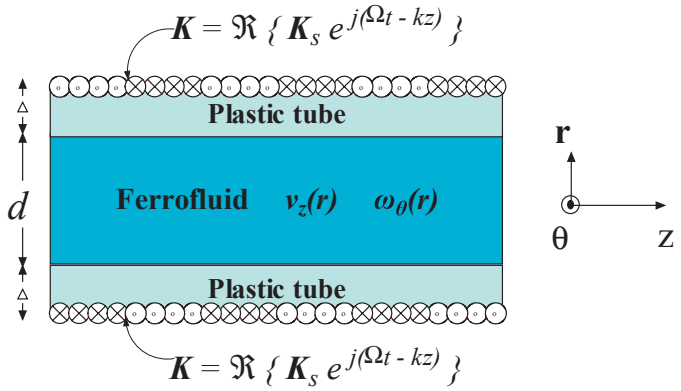

Figure 1: A ferrofluid segment inside a cylinder is magnetically stressed by a spatially traveling sinusoidal current sheet.

2.2. Fluid mechanics

For incompressible fluids

$$\nabla \cdot \mathbf{v} = 0 \quad \nabla \cdot \boldsymbol{\omega} = 0 \tag{3}$$

where $\mathbf{v}$ is linear fluid velocity and $\boldsymbol{\omega}$ is particle angular velocity. The coupled linear and angular momentum conservation equations for force density $\mathbf{f}$ and torque density $\mathbf{T}$ for a ferrofluid are[1]

$$\rho\left[\frac{\partial \mathbf{v}}{\partial t} + (\mathbf{v}\cdot\nabla)\,\mathbf{v}\right] = -\nabla p + \mathbf{f} + 2\zeta\nabla\times\boldsymbol{\omega} + (\zeta+\eta)\,\nabla^2\mathbf{v} \tag{4}$$

$$I\left[\frac{\partial \boldsymbol{\omega}}{\partial t} + (\mathbf{v}\cdot\nabla)\,\boldsymbol{\omega}\right] = \mathbf{T} + 2\zeta\,(\nabla\times\mathbf{v} - 2\boldsymbol{\omega}) + \eta^{'}\nabla^2\boldsymbol{\omega} \tag{5}$$

where ρ is the mass density, p is the pressure, ζ is the vortex viscosity, η is dynamic viscosity, I is the moment of inertia density, and $\eta^{'}$ is the shear coefficient of spin viscosity. At steady-state, without inertial effects, equations (4) and (5) in cylindrical coordinates become

$$(\zeta+\eta)\left(\frac{d^2v_z}{dr^2} + \frac{1}{r}\frac{dv_z}{dr}\right) + 2\zeta\left(\frac{d\omega_\theta}{dr} + \frac{\omega_\theta}{r}\right) - \frac{dp}{dz} + \langle f_z\rangle = 0 \tag{6}$$

$$\eta^{'}\left(\frac{d^2\omega_\theta}{dr^2} + \frac{1}{r}\frac{\omega_\theta}{dr} - \frac{\omega_\theta}{r^2}\right) - 2\zeta\left(\frac{dv_z}{dr} + 2\omega_\theta\right) + \langle T_\theta\rangle = 0 \tag{7}$$

2.3. Magnetic field calculation

The traveling wave current sheet in Figure 1 introduces a traveling wave magnetic field inside the cylindrical channel. Because of symmetry, there is no θ component of the magnetic field. Therefore, the total magnetic field $\mathbf{H}$, the magnetization $\mathbf{M}$ and the magnetic flux density $\mathbf{B}$ inside the ferrofluid are given by

$$\begin{aligned} \mathbf{H} &= \Re\left\{\left(\hat{H}_r(r)\mathbf{i_r}+\hat{H}_z(r)\mathbf{i_z}\right)\cdot e^{j(\Omega t-kz)}\right\}, \quad \mathbf{M}=\Re\left\{\left(\hat{M}_r(r)\mathbf{i_r}+\hat{M}_z(r)\mathbf{i_z}\right)\cdot e^{j(\Omega t-kz)}\right\} \\ \mathbf{B} &= \Re\left\{\left(\hat{B}_r(r)\mathbf{i_r}+\hat{B}_z(r)\mathbf{i_z}\right)\cdot e^{j(\Omega t-kz)}\right\} \end{aligned} \tag{8}$$

where Ω is the frequency of the traveling wave, and k is its wave number.

We would like to solve for $\hat{M}_r$ and $\hat{M}_z$ in terms of the field amplitudes $\hat{H}_r$ and $\hat{H}_z$. Substituting (8) into (1) relates the magnetization components to the magnetic field $\mathbf{H}$. We then solve for $\hat{M}_r$ and $\hat{M}_z$ to obtain

$$\hat{M}_r = \chi_0\frac{\left\{\left[j\left(\Omega\tau-kv_z\tau\right)+1\right]\hat{H}_r+\omega_\theta\tau\hat{H}_z\right\}}{\left[j\left(\Omega\tau-kv_z\tau\right)+1\right]^2+\left(\omega_\theta\tau\right)^2} = C(r)\hat{H}_r+D(r)\hat{H}_z \tag{9}$$

$$\hat{M}_z = \chi_0\frac{\left\{-\omega_\theta\tau\hat{H}_r+\left[j\left(\Omega\tau-kv_z\tau\right)+1\right]\hat{H}_z\right\}}{\left[j\left(\Omega\tau-kv_z\tau\right)+1\right]^2+\left(\omega_\theta\tau\right)^2} = -D(r)\hat{H}_r+C(r)\hat{H}_z \tag{10}$$

where

$$C(r)=\chi_0\frac{j\left(\Omega\tau-kv_z\tau\right)+1}{\left[j\left(\Omega\tau-kv_z\tau\right)+1\right]^2+\left(\omega_\theta\tau\right)^2}, \quad D(r)=\chi_0\frac{\omega_\theta\tau}{\left[j\left(\Omega\tau-kv_z\tau\right)+1\right]^2+\left(\omega_\theta\tau\right)^2} \tag{11}$$

In general, $C(r)$ and $D(r)$ are r-position dependent through the position dependence of $\mathbf{v}$ and $\boldsymbol{\omega}$. Within the current-free ferrofluid, Gauss's law for the magnetic flux density and Ampere's law for the magnetic field require the imposed fields to satisfy

$$\nabla\times\mathbf{H}=\mathbf{0}\Rightarrow\hat{H}_r(r)=\frac{j}{k}\frac{d\hat{H}_z(r)}{dr}, \quad \nabla\cdot\mathbf{B}=\mathbf{0}\Rightarrow\frac{1}{r}\frac{\partial}{\partial r}\left[r\cdot\hat{B}_r(r)\right]+\frac{\partial\hat{B}_z(r)}{\partial z}=0 \tag{12}$$

where

$$\mathbf{B}=\mu_0\left(\mathbf{H}+\mathbf{M}\right) \tag{13}$$

Substituting (13) into (12), together with (9) - (11), yields the magnetic field equation

$$\frac{d^2\hat{H}_z(r)}{dr^2}-\left[\frac{1}{1+C(r)}\frac{dC(r)}{dr}+\frac{1}{r}\right]\frac{d\hat{H}_z(r)}{dr}+\left\{\frac{-jk}{1+C(r)}\left[\frac{D(r)}{r}+\frac{dD(r)}{r}\right]-k^2\right\}\hat{H}_z(r)=0 \tag{14}$$

2.4. Magnetic field boundary conditions

In order to solve Equation (14) to determine the magnetic field throughout the ferrofluid, one needs to specify the boundary conditions for the magnetic field equation, which can be done by employing the general magnetic diffusion equation[5]

$$\frac{1}{\mu\sigma}\nabla^2\mathbf{B}=\left(\frac{\partial\mathbf{B}}{\partial t}+\left(\mathbf{v}\cdot\nabla\right)\right)\mathbf{B} \tag{15}$$

Note that the Equation (15) is valid for material layers outside the ferrofluid.

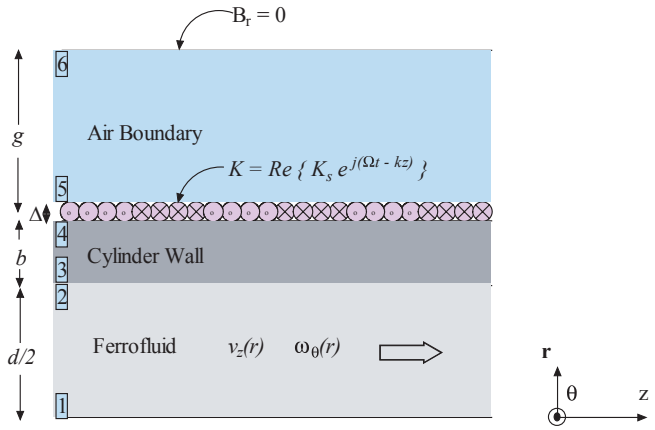

Figure 2: Setup of the multilayered boundary problem. The air layer is taken thick enough to represent an infinite boundary, whereas Δ is infinitesimally small.

In general, for the isotropic material layers shown in Figure 2, one gets the following diffusion transfer relations

$$\begin{pmatrix} \hat{B}_{4,r} \\ \hat{B}_{3,r} \end{pmatrix} = -\frac{j\mu}{k} \begin{pmatrix} f_0\left(d/2, d/2+b\right) & g_0\left(d/2+b, d/2\right) \\ g_0\left(d/2, d/2+b\right) & f_0\left(d/2+b, d/2\right) \end{pmatrix} \begin{pmatrix} \hat{H}_{4,z} \\ \hat{H}_{3,z} \end{pmatrix} \tag{16a}$$

$$\begin{pmatrix} \hat{B}_{6,r} \\ \hat{B}_{5,r} \end{pmatrix} = -\frac{j\mu}{k} \begin{pmatrix} f_0\left(d/2+b+\Delta, d/2+b+g\right) & g_0\left(d/2+b+g, d/2+b+\Delta\right) \\ g_0\left(d/2+b+\Delta, d/2+b+g\right) & f_0\left(d/2+b+g, d/2+b+\Delta\right) \end{pmatrix} \begin{pmatrix} \hat{H}_{6,z} \\ \hat{H}_{5,z} \end{pmatrix} \tag{16b}$$

$$f_0\left(r_\alpha, r_\beta\right) = \frac{k\left[K_0(kr_\alpha)I_0'(kr_\beta) - I_0(kr_\alpha)K_0'(kr_\beta)\right]}{I_0(kr_\alpha)K_0(kr_\beta) - I_0(kr_\beta)K_0(kr_\alpha)} \tag{16c}$$

$$g_0\left(r_\alpha, r_\beta\right) = \frac{1}{r_\alpha\left[I_0(kr_\alpha)K_0(kr_\beta) - I_0(kr_\beta)K_0(kr_\alpha)\right]} \tag{16d}$$

Here μ is the material's magnetic permeability, k is the wave number, and $\hat{H}_z$ is the complex amplitude of the z-directed magnetic field at the surface indicated by the numeric subscript. I_0 and K_0 are the modified Bessel functions[5]. The field boundary conditions at the material interface are

$$B_{5,r} = B_{4,r}, \quad B_{6,r} = H_{6,z} = 0, \quad H_{4,z} - H_{5,z} = K_s \tag{17}$$

Once Equations (16) and (17) are solved, one can find the complex field amplitude at each boundary surface as a function of the amplitude, K_s, of the traveling wave current sheet at the outer tube wall.

2.5. Magnetic force and torque densities

For $0 \le r \le d/2$, *i.e.*, inside the ferrofluid, the magnetic force density is[4]

$$\mathbf{f} = \mu_0\left(\mathbf{M}\cdot\nabla\right)\mathbf{H} \tag{18}$$

The time average components of the force density are then given by

$$\langle f_r\rangle = \frac{1}{2}\mu_0\Re\left[\hat{M}_r\frac{d\hat{H}_r^*}{dr} + jk\hat{M}_z\hat{H}_r^*\right], \quad \langle f_z\rangle = \frac{1}{2}\mu_0\Re\left[\hat{M}_r\frac{d\hat{H}_z^*}{dr} + jk\hat{M}_z\hat{H}_z^*\right] \tag{19}$$

The torque density inside the ferrofluid is given by[4]

$$\mathbf{T} = \mu_0 \left(\mathbf{M} \times \mathbf{H} \right) \tag{20}$$

The torque has only a θ-directed component, so the time average of torque density is

$$\langle T_\theta \rangle = \frac{1}{2} \mu_0 \Re \left[-\hat{M}_r \hat{H}_z^* + \hat{M}_z \hat{H}_r^* \right] \tag{21}$$

3. SOLUTION METHOD

Equations (6) and (7) are numerically solved by an iterative method with a second-order central-differencing scheme. First, initial estimates of $\mathbf{v}$ and $\boldsymbol{\omega}$ are made to calculate H_z and H_r by using Equation (14); then, force density $\mathbf{f}$ and torque density $\mathbf{T}$ are determined from Equations (19), (20) and (21). After that, new sets of $\mathbf{v}'$ and $\boldsymbol{\omega}'$ are obtained by solving Equation (6) and (7). We compare the new $\mathbf{v}'$ and $\boldsymbol{\omega}'$ with previous values; if the norm of the difference is larger than a preset tolerance, $\mathbf{v}'$ and $\boldsymbol{\omega}'$ become the new estimates, and the iteration continues till the tolerance criterion is met.

4. DISCRETIZATION METHOD

Figure 3 shows the discretization scheme with n unit cells across the radial distance. Within each unit cell, flow velocity, spin velocity and magnetic field values are constant. Discretizing the magnetic field Equation (14) in this scheme yields

$$\hat{H}_z(r)\Big|_{r=(i-1)\Delta r+\frac{\Delta r}{2}} = \hat{H}_{z,i}, \quad \frac{d\hat{H}_z(r)}{dr}\Big|_{r=(i-1)\Delta r+\frac{\Delta r}{2}} = \frac{\hat{H}_{z,i+1}-\hat{H}_{z,i-1}}{2\Delta r} \tag{22}$$

$$\frac{d^2\hat{H}_z(r)}{dr^2}\Big|_{r=(i-1)\Delta r+\frac{\Delta r}{2}} = \frac{\hat{H}_{z,i+1}+\hat{H}_{z,i-1}-2\hat{H}_{z,i}}{(\Delta r)^2} \tag{23}$$

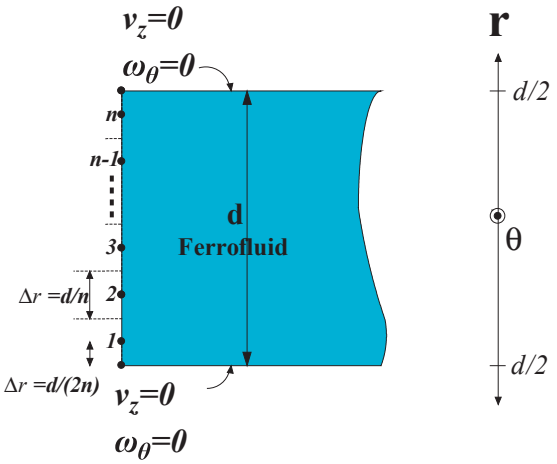

Figure 3: Discretization in the r-direction. Within each unit cell, the flow velocity v_z, spin velocity ω_θ and the z-component magnetic field strength $\hat{H}_z$ are assumed to be constant.

The discretized Equation (14) is of the form

$$a_{H,i+1}\hat{H}_{z,i+1} + a_{H,i}\hat{H}_{z,i} + a_{H,i-1}\hat{H}_{z,i-1} = 0 \tag{24}$$

where

$$a_{H,i+1} = \frac{1}{(\Delta r)^2} + \frac{1}{2\Delta r}\left[1 + \frac{1}{1+C_{i+1}}\left(\frac{dC}{dr}\right)_{i+1}\right] \tag{25a}$$

$$a_{H,i} = -\frac{2}{(\Delta r)^2} + \left[\frac{-jk}{1+C_i}\left(\frac{D_i}{r}\frac{dD}{dx}\right)_i - k^2\right] \tag{25b}$$

$$a_{H,i-1} = \frac{1}{(\Delta r)^2} + \frac{1}{2\Delta r}\left[1 + \frac{1}{1+C_{i-1}}\left(\frac{dC}{dr}\right)_{i-1}\right] \tag{25c}$$

Note that C, D, dC/dr and dD/dr are evaluated numerically using the $\mathbf{v}$ and $\boldsymbol{\omega}$ values from the previous iteration. Similarly, discretizing Equations (6) and (7) gives

$$m_{v,i+1}v_{z,i+1} + m_{v,i}v_{z,i} + m_{v,i-1}v_{z,i-1} + m_{\omega,i+1}\omega_{\theta,i+1} + m_{\omega,i}\omega_{\theta,i} + m_{\omega,i-1}\omega_{\theta,i-1} = b_{m,i} \tag{26a}$$

$$n_{v,i+1}v_{z,i+1} + n_{v,i}v_{z,i} + n_{v,i-1}v_{z,i-1} + n_{\omega,i+1}\omega_{\theta,i+1} + n_{\omega,i}\omega_{\theta,i} + n_{\omega,i-1}\omega_{\theta,i-1} = b_{n,i} \tag{26b}$$

where

$$\begin{aligned}
m_{v,i+1} &= (\eta+\zeta)\left[\frac{1}{(\Delta r)^2} + \frac{1}{(2i-1)(\Delta r)^2}\right] \quad , \quad m_{v,i} = -\frac{2(\eta+\zeta)}{(dr)^2} \\
m_{v,i-1} &= (\eta-\zeta)\left[\frac{1}{(\Delta r)^2} + \frac{1}{(2i-1)(\Delta r)^2}\right] \quad , \quad m_{\omega,i+1} = \frac{\zeta}{\Delta r} \\
m_{\omega,i} &= \frac{2\zeta}{(i-\frac{1}{2})\Delta r}, m_{\omega,i-1} = -\frac{\zeta}{\Delta r}, b_{m,i} \;=\; -\langle f_z\rangle_i + \frac{dp}{dz} \\
n_{v,i+1} &= -\frac{\zeta}{\Delta r} \quad , \quad n_{v,i} = 0, \quad n_{v,i-1} = \frac{\zeta}{\Delta r}
\end{aligned} \tag{27}$$

$$\begin{aligned}
n_{\omega,i+1} &= \eta'\left[\frac{1}{(\Delta r)^2} + \frac{1}{(2i-1)(\Delta r)^2}\right] \quad , \quad n_{\omega,i} = \frac{2\eta'}{(\Delta r)^2} - \eta'\frac{1}{\left[(i-\frac{1}{2})(\Delta r)\right]^2} \\
n_{\omega,i-1} &= \eta'\left[\frac{1}{(\Delta r)^2} - \frac{1}{(2i-1)(\Delta r)^2}\right] \quad , \quad b_{n,i} = -\langle T_\theta\rangle_i
\end{aligned} \tag{28}$$

5. RESULTS AND DISCUSSION

In the real physical system, the spin viscosity η' is typically very small but nonzero[6]. The ferrofluid flow velocity and magnetic particle spin profiles inside a cylinder are shown in Figure 4. Note that non-slip boundary conditions for both $\mathbf{v}$ and $\boldsymbol{\omega}$ are satisfied, except when η' = 0. To obtain the ferrofluid flow and spin profiles in the small spin viscosity case, we simply set the spin viscosity $\eta' = 0$, which reduces the governing Equations (6) and (7) to a second order system. Corresponding results are shown in Figure 4. The parameters in Figure 4 are chosen to correspond to those of a commercially available, oil-based ferrofluid.

Traveling wave magnetic fields develop both magnetic body force and torque pumping. Figure 5 shows the pumping effect due to each effect, as well as the total pumping.

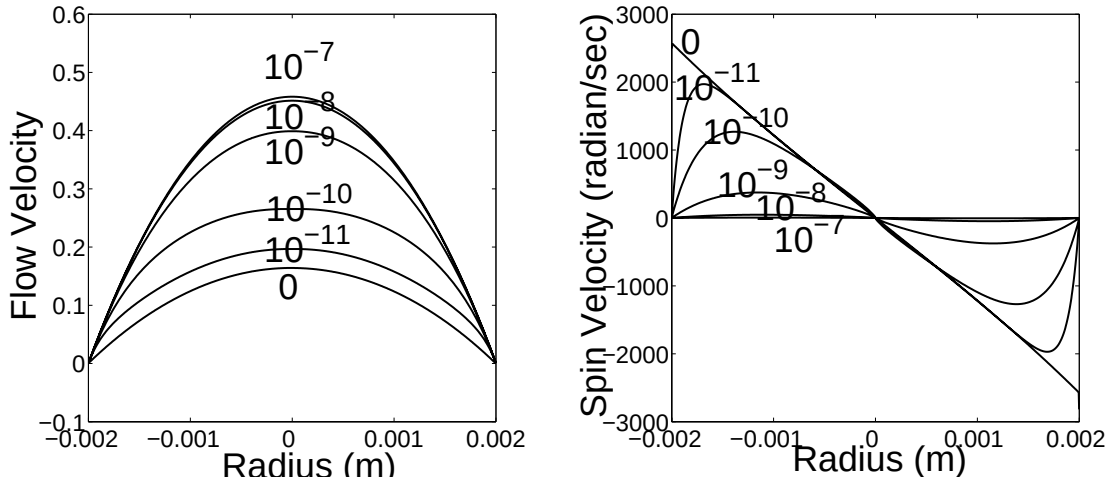

(a) Flow velocity (b) Particle angular velocity

Figure 4: Flow velocity (a) and particle angular velocity (b) for various spin viscosity $\eta^{'}$ values. Current sheet density = 10000 A/m, excitation frequency = 50 kHz, radius of cylinder r = 2 mm, traveling wave period T = 12.6 mm, $\chi_0 = 1.7$, $\tau = 10\ \mu s$, $\eta = 0.006$ Kg/m.s, $\zeta = 0.00081$ Kg/m.s, $\eta^{'}$ = 0,10^{-11},10^{-10},10^{-9},10^{-8},10^{-7} Kg/m.s, $dp/dz = 0$, the wall thickness is negligible.

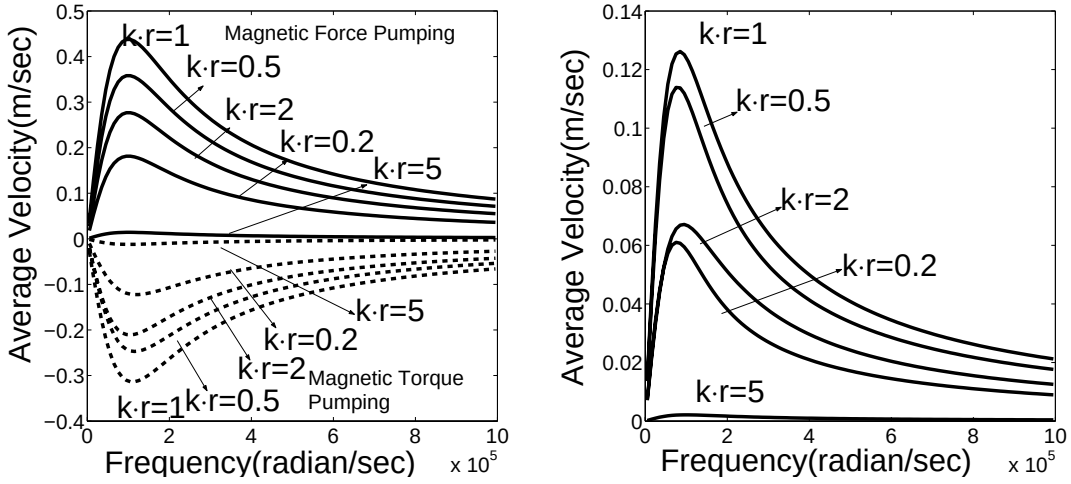

(a) Magnetic torque, force pumping only (b) Magnetic torque and force pumping

Figure 5: Pumping due to magnetic force only (solid lines in a) and torque (dashed lines in a) only, and both (b) for various traveling wave periods. Current sheet density = 10000 A/m, radius of cylinder r = 2 mm, wave number k = $2\pi/T$, traveling wave period T = 1.3 mm, 2.5 mm, 6.3 mm, 12.6 mm, 25.1 mm, 62.8 mm. Other properties are the same as those in Figure 4.

Average flow velocities for various traveling wave periods and magnetic field frequencies are shown in Figure 6. The flow velocity is strongly dependent on the traveling wave period. Maximum flow velocity is achieved when the product of the excitation wave number and radius of the ferrofluid cylinder approaches unity. Once geometric dimensions are chosen, the flow velocity can be precisely controlled by the applied magnetic field frequency. As shown in Figure 6, maximum flow velocity is achieved when the applied magnetic field frequency is close to the reciprocal of the relaxation time constant of magnetic particles

inside the ferrofluid.

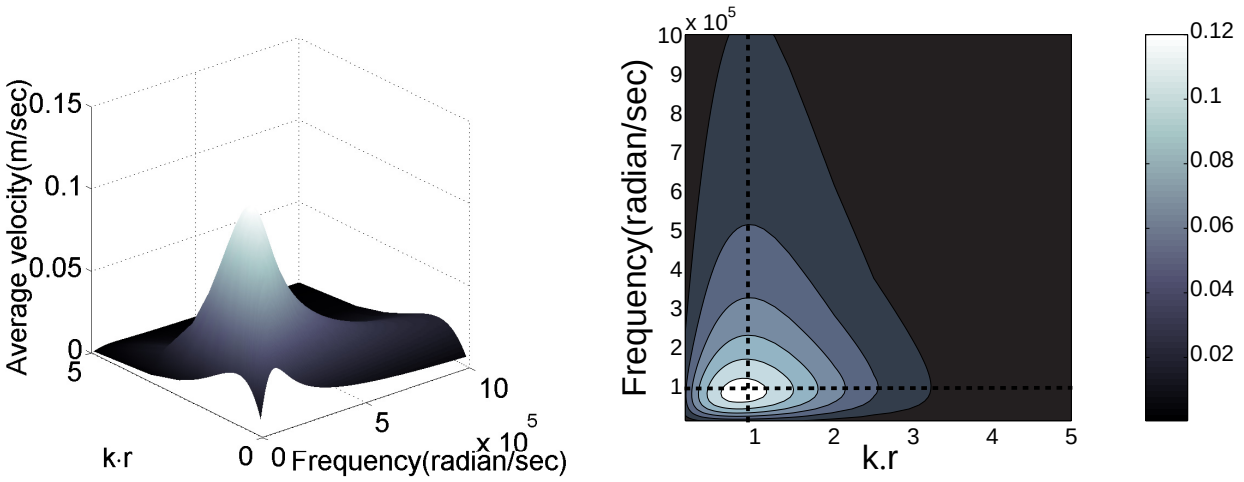

(a) Average velocity vesus magnetic field frequency and $k \cdot r$

(b) Contour plot of average velocity vesus magnetic field frequency and $k \cdot r$

Figure 6: 3-D (a) and contour (b) plot of average flow velocity of ferrofluid versus the product of wave number and radius of ferrofluid cylinder $k \cdot r$ for various applied magnetic field frequency. Maximum pumping is achieved when the product is approximately unity. Pumping efficiency increases as the applied magnetic field frequency becomes comparable to the reciprocal of the relaxation time constant of magnetic particle in the ferrofluid. Same material properties and operating conditions as in Figure 4.

6. CONCLUSION

In this work, a numerical method to solve ferrofluid dynamics in spatially-traveling, sinusoidally time-varying magnetic fields has been developed. Simulation results show that magnetic torque pumping due to traveling wave is opposite in direction and smaller in magnitude than magnetic body force pumping due to field gradients. Maximum flow velocity is achieved when the product of the excitation wave number and the radius of the ferrofluid channel approaches unity, and the excitation frequency is close to the reciprocal of the relaxation time constant of magnetic particles.

ACKNOWLEDGEMENT

We thank Professor Markus Zahn for insightful discussions and his useful advice.

REFERENCES

[1] R. E. Rosensweig, Ferrohydrodynamics (Cambridge University Press, U.K.).

[2] K. Raj and R. Moskowitz, J. of Magnetism and Magnetic Materials **85** (1990) 233.

[3] Y. Haik, V. N. Pai, C. J. Chen, J. of Magnetism and Magnetic Materials **225** (2001) 180.

[4] M. Zahn and D. R. Greer, J. of Magnetism and Magnetic Materials **149** (1995) 165.

[5] J.R. Melcher, Continuum Electromechanics (MIT Press, Cambridge, MA, U.S.).

[6] Kristopher R. Schumacher, Inga Sellien, G. Stuart Knoke and Tahir Cader, Physical Review E **67** (2003) 026308.